Comparison of Performance Base and Optimized Blades of Horizontal Axis Wind Turbine

M.R. Saber*, M.H.Djavareshkian*‡

*Department of Mech. Engg., Faculty of Engg., Ferdowsi University of Mashhad, Mashhad, Iran

(mrs_mechanic@yahoo.com , javareshkian@um.ac.ir)

‡ Corresponding Author; M.H.Djavareshkian, Mechanical Engineering Department., Faculty of Engineering., Ferdowsi University of Mashhad, Mashhad, Iran M.H. Djavareshkian, +98 511 880 5037, javareshkian@um.ac.ir

Received: 02.12.2013 Accepted: 14.01.2014

Abstract- In this study, the results of two optimized and base blades of a horizontal axis wind turbine with aerodynamic point of view and analyze the stresses and strains are compared. The aerodynamic forces are obtained by solving the viscous flow and the optimization is done by genetic algorithm and neural network. By applying the aerodynamic loads, the stress and strain are analyzed. In order to optimization, the chord length and the twist angle of the blade at various radiuses have been calculated by BEM. The Navier Stokes equations are solved to simulate both two and three dimensional flows. The Results which are obtained from 2D Computational Fluid Dynamics (CFD) have been utilized to train a Neural Network (NN). In the process of airfoil optimization, Genetic Algorithm (GA) is coupled with trained NN to attain the best airfoil shape at each angle of the attack. First, the results of both optimized and base wing are compared then the aerodynamic forces on the blades were applied for stress analysis. The results of the analysis of the stress - strain showed that optimized wing improves the wing performance.

Keywords- BEM, Genetic Algorithm, Neural Network, Optimization.

1. Introduction

Power of tapping from wind energy systems has high impact on the economic analysis of this type of energy and capture energy from the wind turbine dependents the blade design and the relevant factors. Wind turbines are exposed to various stresses and loads, and due to the nature of the wind, the loads are highly variable. Design for dynamic loading compared with static loading, due to the emergence of the phenomenon of fatigue is much harder. Since experimental studies are very expensive and time consuming, and also, because of the complex geometry, and analytical methods are lacking in this case, the perfect solution is using numerical methods. In other words, one of the suitable methods to evaluate a new design of wind turbine blades is the numerical modeling. Min Soo Jeonga and colleagues [1] in 2013 evaluated the impact of yaw error on aero-elastic characteristics of a horizontal axis wind turbine blade based on blade element momentum theory. The results of this study showed that the amount of aero-elastic damping in the worst case can be reduced to 33 percent. Jong-Won Leea and colleagues [2] in 2012, evaluated the performance characteristics aero-elastic wind turbine blades based on flexible body dynamics by ANSYS software, and the results were compared with experimental results NREL. Cardenasa and colleagues [3] in 2012, evaluated the extent and location of damage to the blades of turbine by using a combined approach, reduced-order and simplify to the thin beam model. Hoogedoorna [4] in 2008, paid to the aero-elastic behavior of a flexible blade for wind turbine. This code uses a combination of X-foil software for aerodynamic analysis and solids analysis was performed by MATLAB and the impact of the flexible airfoil on the design parameters investigated. Baxevanoua [5] in 2008, using a new numerical model of aero-elastic resulting from the solution of the Navier-Stokes models with elastic model and two scheme combines to study of behavior aero-elastic in the wings flutter and they began to study various parameters on the blade. Freno [6] in 2011, used an effective computational method for nonlinear analysis of a wind turbine blade. He approximated turbine blade with a non-uniform cantilever beam that reduce the computational cost of the analysis.

Puterbaugh [7] in 2011, examined dependent parameters of wind turbine blades with a flexible elastic material. He used a mathematical model to predict the amount of deformation caused by aerodynamic forces on wind turbine blades, the results showed that a non-prismatic beam can be approximated with an airfoil. Monte [8] in 2013, paid to solid geometry optimization by using multi-objective Genetic Algorithms on wind turbine blades with composite materials that will reduce the weight and increase the strength of the edges. Chena and colleagues [9] in 2013, began to study the optimization of solid geometry in wind turbine, that in this method uses a hybrid approach based on blade element theory and particle swarm algorithm for the optimization of the blade that this method reduces the weight of the rotor blades and the mass density. Buckney and colleagues [10] in 2013, paid to optimization of wind turbine blades using topology optimization techniques. They were able to reach maximum hardness and minimum stresses in the blades with this method. Results showed that in this method, the blade worked more efficiently in asymmetrical bending.

In almost all of researches has been done, a series of assumptions to simplify the analysis and modeling has been used. And less attention to aerodynamic optimization and analysis of stress-strain simultaneously, has been done. Djavareshkian and colleagues [11] was optimized wind turbine blade with solving the Navier-Stokes and Genetic Algorithms and Neural Networks. The aim of this study was to compare the optimized turbine blade and the base of axial wind turbine blade and aero-elastic analysis as above. In this study, after comparing the aerodynamic blades, the forces apply on the blade grid nodes and stress analysis do by ANSYS software. At the beginning of the study, the results have been validated for aerodynamic analysis and stress, then with the placement of aerodynamic forces on the blade grid nodes, stress, strain and displacement were extracted and were compared.

2. Methodology

2.1. Governing Equation and Discretization

The basic equations which describe the conservation of mass, momentum and scalar quantities can be expressed in the following vector forms which are independent in the coordinate system. In this study, $k-\varepsilon$ model is utilized for turbulence flow. These equations are discretized by finite volume method and terms of displacement by using dimensionless variables are controlled and limited. Discrete equations are solved by SIMPLE algorithm. In order to optimize the Neural Networks and Genetic Algorithm, and algorithm BEM for data processing has been applied. Further details of the discrete equations, the algorithm solves the fluid flow, and aerodynamic optimization algorithm in reference [11] is given. For stress analysis of two blades, stiffness or displacement method was used for the analysis of the stress-strain. In this method, the unknowns are the nodal displacements. Considering the Compatibility and Equilibrium equations at each node, we will obtain a set of algebraic equations that will be arranged in terms of the unknown nodal displacements. Using the equations of Equilibrium, relation between forces and displacements are calculated and by obtaining a algebraic equations device and solve it, the displacement of nodes are calculated [12]. The three-dimensional equilibrium equations can be written as follows.

$$\begin{aligned}
&\frac{\partial \sigma_x}{\partial x}+\frac{\partial \tau_{xy}}{\partial y}+\frac{\partial \tau_{xz}}{\partial z}+F_x=0\\
&\frac{\partial \sigma_y}{\partial y}+\frac{\partial \tau_{xy}}{\partial x}+\frac{\partial \tau_{yz}}{\partial z}+F_y=0\\
&\frac{\partial \sigma_z}{\partial z}+\frac{\partial \tau_{xz}}{\partial x}+\frac{\partial \tau_{yz}}{\partial y}+F_z=0
\end{aligned} \tag{1}$$

Equations strain–displacement for a cube element with the dimensions dx, dy and dz is as follows. Where v, u and w are the displacements in the direction of the coordinate axis.

$$\begin{aligned}
&\varepsilon_x=\frac{\partial u}{\partial x}\ ,\ \varepsilon_y=\frac{\partial v}{\partial y}\ ,\ \varepsilon_z=\frac{\partial w}{\partial z}\\
&\gamma_{xy}=\frac{\partial u}{\partial y}+\frac{\partial v}{\partial x}\ ,\gamma_{yz}=\frac{\partial v}{\partial z}+\frac{\partial w}{\partial y},\gamma_{zx}=\frac{\partial w}{\partial x}+\frac{\partial u}{\partial z}
\end{aligned} \tag{2}$$

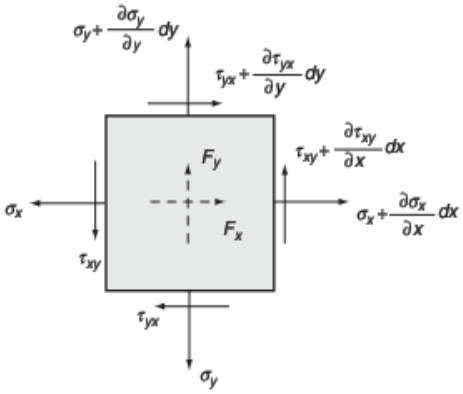

Fig .1. Elements of a two-dimensional stress state

Equations stress-strain is also below.

$$\begin{aligned}
&\sigma_x=2\,G\,\varepsilon_x+\lambda\,e \quad \tau_{xy}=G\,\gamma_{xy}\\
&\sigma_y=2\,G\,\varepsilon_y+\lambda\,e \quad \tau_{yz}=G\,\gamma_{yz}\\
&\sigma_z=2\,G\,\varepsilon_z+\lambda\,e \quad \tau_{xz}=G\,\gamma_{xz}
\end{aligned} \tag{3}$$

In which:

$$e=\varepsilon_x+\varepsilon_y+\varepsilon_z \tag{4}$$

$$\lambda=\frac{v\,E}{(1+V)(1-2\,V)} \tag{5}$$

In the above equations, σ normal stress, τ shear stress, ε vertical strain, γ shear strain, respectively. The shear modulus G and the value of λ, called the Lame constants. e indicating dilatation strain or change of volume per unit volume [13]. By solving these equations with fifteen unknown parameters in three-dimensional elasticity problems can be solved. At first, it can be obtained the geometrical model combination of points, lines, surfaces and volumes. In most finite element software for geometric models can be created by the software itself, or the geometric models created in other software environments that calling. Here the wind turbine blade geometry is optimized by

Genetic Algorithm and Neural Network, is built on Solid works software. Fig .2 shows the model geometry.

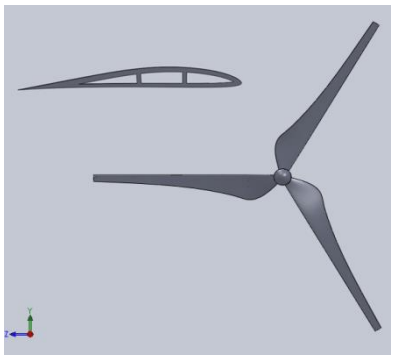

Fig.2. Geometric model of wind turbine blades

Boundary conditions used in this simulation consists of fixed nodes on the main axis wind turbine rotor and the non-rotating in the direction perpendicular to the axis of rotation of these nodes. In this simulation, in addition to exert compressive forces result of solving Computational Fluid Dynamics, the inertial force resulting from the rotation of the turbine blades is also considered. Here the wind speed is 20 meters per second, and the rotational speed of the turbine is 8.235 radians per second. Grid and the aerodynamic forces exerted on nodes of blades in Fig.3 are shown. For the numerical solution of geometry in form of the finite element is necessary to obtain the stiffness matrix of each element. With obtaining the stiffness matrix, equations governing the behavior of an element is obtained as follows:

$$\{f\}^e = [k]^e \{d\}^e \quad (6)$$

Where, $\{f\}^e$ vector of element nodal forces, $[K]^e$ element stiffness matrix, $\{d\}^e$ is a vector of element nodal degrees of freedom, respectively.

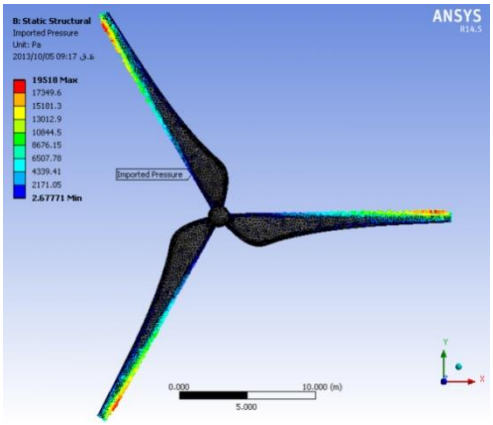

Fig.3. Mesh and aerodynamic forces on the turbine blade nodes

By using superposition of elements stiffness matrices, general stiffness matrix is obtained. Below relations, for superposition principle of stiffness matrix elements, nodal force vector elements and vector degrees of freedom are written.

$$[k] = \sum_{e=1}^{n}[k]^e, \{f\} = \sum_{e=1}^{n}\{f\}^e, \{d\} = \sum_{e=1}^{n}\{d\}^e \quad (7)$$

As a result, the general equation of the following form is obtained:

$$\{f\} = [k]\{d\} \quad (8)$$

Where, {f}, [k] and {d} are nodal force vector of the structure, stiffness matrix of the structure and the vector of nodal degrees of freedom of the structure, respectively. In writing the above equation, the boundary conditions are exerted. In this step the general equation solve with the method of Gauss-Seidle and displacement of d_i are calculated. The calculated d_i is using in equations strain–displacement and stress-strain then, the stress and strain are calculated for each element.

2.2. Boundary Condition

Three-dimensional geometry of the boundary conditions for the above are as follows.

- Fixed nodes on the main axis wind turbine rotor and the non-rotating in the direction perpendicular to the axis of rotation of this nodes.
- Applying compressive forces resulting from solving Computational Fluid Dynamics.
- Applying the inertial force resulting from the rotation of the turbine blades.

2.3. Procedures

2.3.1. Blade Profile Design

The chord profile and twist angle of the blade have been determined at each cross section of the blade by BEM method. The absolute angles of attack at some radiuses are calculated because it varies locally alongside the blade.

2.3.2. Airfoil Optimization

The GA is coupled with CFD to create and analyze many airfoils. The results of numerical simulation are utilized to train various NN architectures. When several NN architectures are examined, then the network architecture with lower MSE is elected as trained NN. In the present research, the training process is separated from optimization procedure. Further details of the algorithm to solve fluid flow and aerodynamic optimization algorithm in [11] are given.

3. Results and Discussion

First, bring a brief of the results of computational fluid dynamics in the blade optimized and base then the results of the stress analysis will be given.The base airfoil which is applied for optimization process is E387 Eppler. The blade length is equal to 16.24m. The tip speed ratio (TSR) is 7 which mean angular velocity is 6.17 rad/s. The wind speed is considered 15m/s. The angle of attack varies from -2.5 to 20.04 degrees and average Reynolds number of the flow is 4500000. The validation of numerical results with experimental data has been done.The validation of 3D simulations has been carried out by comparing the numerical results with NREL phase VI wind turbine rotor. The pressure

coefficient in 50% of the radius of blade is illustrated in Fig.4.

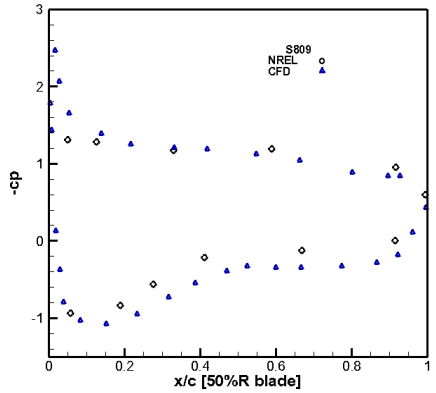

Fig.1. The pressure coefficient of the experiment data NREL phase VI and numerical result at 50% of the blade

This comparison shows that there is a difference between these two results. This difference could be due to several parameters such, turbulent, separation phenomenon, wakes in downwind of the wind turbine, rotation of the blades and tip vorticesthat are not well predicted by the numerical simulation. Shape of optimized airfoils in respect to base airfoil at some angles of attack is illustrated in Fig.5. This figure shows that the airfoils at higher angles of attack are thicker because this postpones the separation. The comparison of pressure coefficient for both wind turbines, in spanwise direction are presented in Fig. and Fig.. Power factor with respect to tip speed ratio is illustrated in Fig.. This figure confirms considerable improvement in power factor.

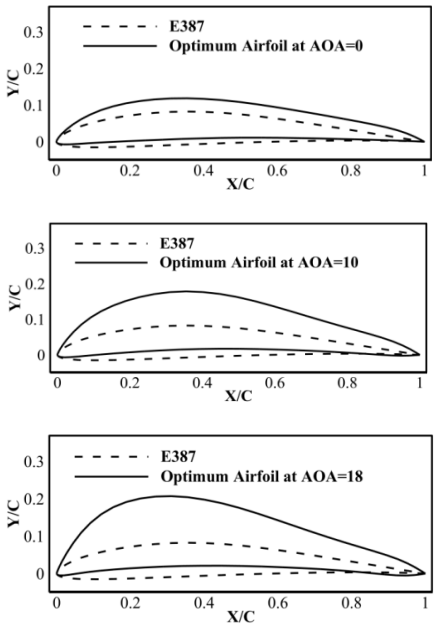

Fig. 5. The shape of smart airfoil in respect to base airfoil at each AOA

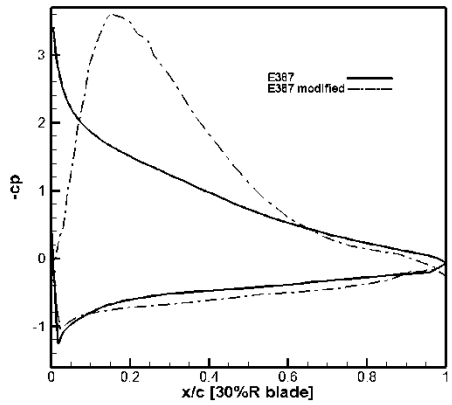

Fig.6. The pressure coefficient of base and optimized wind turbine in 30% of the blade , 15m/s

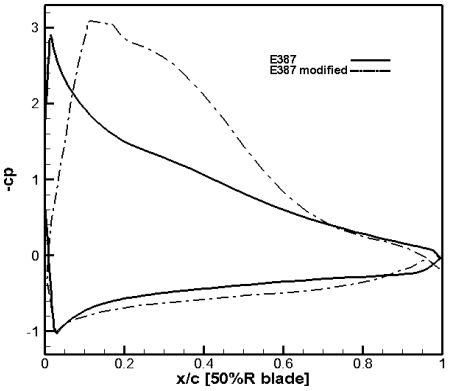

Fig.7. The pressure coefficient of base and optimized wind turbine in 50% of the blade , 15m/s

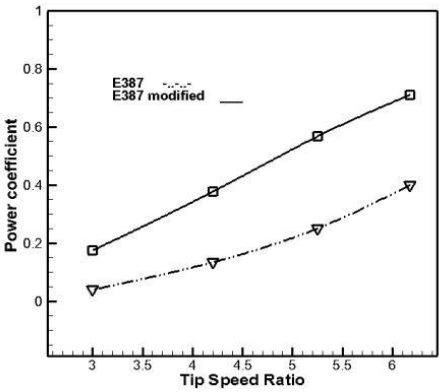

Fig.8. The power factor with respect to tip speed ratio

These curves show that significant changes after optimizing in pressure distribution is created. Optimized blades relative to the baseline, creates more pressure on each sides of blades and causes the blade produce more power.

3.1. Material Properties Used

Material properties used in this study in Table.1 is shown.

Table 1. Properties of materials

Density	1500 kg / m^3
Coefficient of Thermal Expansion	1.2E-5 *1/c*
Specific Heat	434 *J / kg.c*
Thermal Conductivity	60.5 *W / m.c*
Resistivity	1.7E-7 *ohm m*
Young's Moodulus	1.9E11 *Pa*
Poisson's Ratio	0.3
Bulk Modulus	1.5833E11 *Pa*
Shear Modulus	7.3077E10 *Pa*
Compressive Yield Strength	3.7E8 *Pa*
Tensile Yield Strength	3.5E8 *Pa*
Tensile Ultimate Strength	4.6E8 *Pa*

The purpose of the analysis is that the stress and strain analysis be done on the blades. Now we want to examine whether the optimized blade, has the ability to withstand the aerodynamic loads? What is the reliability of wind turbine rotor? And the maximum principal stress in the rotor blades is not higher than the yield stress. In order to validate wind turbine blade in stress analysis, at first, blade approximated with a cantilever beam, and non-uniform compressive force applied to the beam, and the numerical results are compared with the exact solution. Non-uniform compressive force on the beam is shown in Fig.9 . Length of the beam 10 m and its cross-sectional size 0.2 m in width and 0.5 in height. The following calculations to obtain the maximum stress and displacement end of beam with exact solution, have been performed. Fig. 10 shows the comparison of analytical (Eq. 9,10,11,12) and numerical displacement along the beam.

$$y'' = \frac{M_{(x)}}{E\,I} \quad , \quad y'(0) = 0 \quad , \quad y(0) = 0 \tag{9}$$

$$M_{(x)} = -6666.66 + 1000\,x - 3.3333\,x^3 \tag{10}$$

$$\begin{cases} y' = \int y''\,dx = \dfrac{1}{E\,I}[-6666.66x + 500\,x^2 - 0.8333\,x^4] \\ y = \int y'\,dx = \dfrac{1}{E\,I}[-3333.333\,x^2 + 166.66\,x^3 - 0.1666\,x^5] \end{cases} \tag{11}$$

$$\begin{cases} y_{(10)} = 0.00044\ \text{m} \\ \sigma_{Max} = \dfrac{y.M_{(x)}}{I} = 1.6\text{MPa} \quad , \quad E = 200\text{GPa} \end{cases} \tag{12}$$

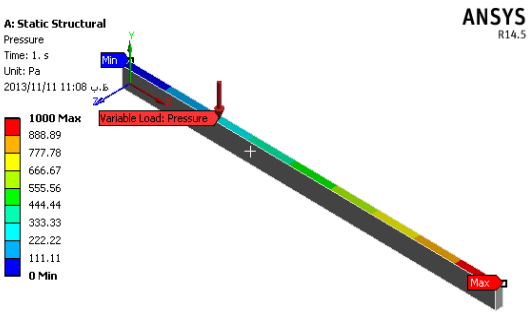

Fig.9. Non-uniform compressive force on the beam

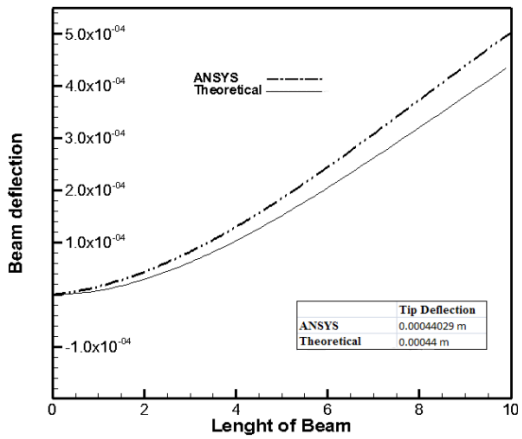

Fig.10. Comparison of theory and numerical displacement along the beam

In the following figures, at first , the deformation due to aerodynamic forces including drag and lift are shown. For this purpose, the blade deformation diagrams are drawn in different directions and the base and optimized blades, are compared with each other. Finally, the von Mises stress, maximum shear stress, normal strain and factor of safty of the blade, are shown. Figs. 11 and 12 show the results of deformation by a force along the axis of rotation for the base and optimized blades respectively.

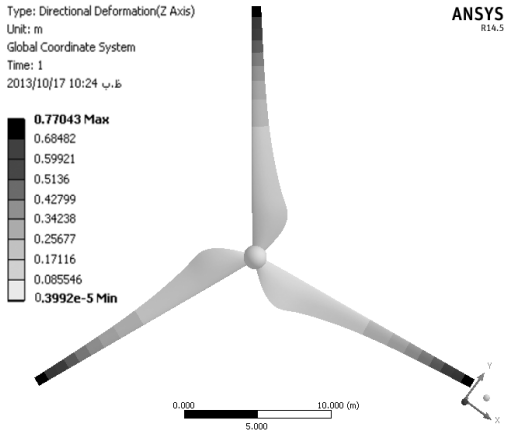

Fig.11. Results deformed by a force along the axis of rotation to the blade base

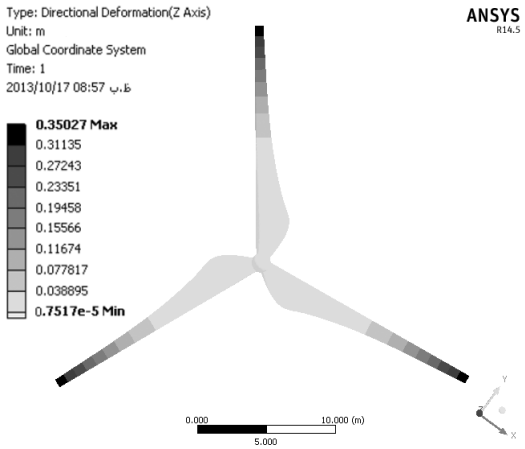

Fig.12. Results deformed by a force along the axis of rotation the optimized blade

Fig.13 shows the deformation of two mention blades along the axis of rotation. It is seen that, with increasing radius, displacement of optimized blade is lower.

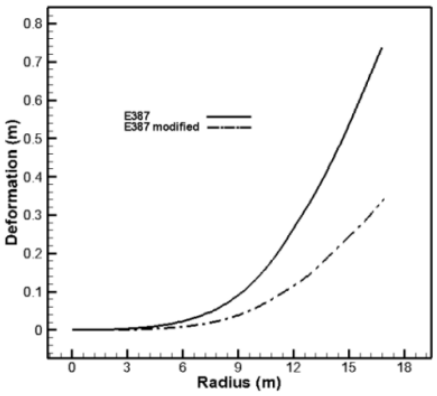

Fig.13. deformations of two blades along the axis of rotation

In other words, displacement in the tip of optimized blade is approximately 35 cm and in base blade about 77 cm which indicates that, deformation at the tip of optimized blade compared with the base blade is about 42 cm .This shows that ,the bending moment is less in optimized blade and also causes optimized blade geometry, has smaller changes. Also the aerodynamic forces on the blade is less changes. Low deformation, less power can be reduced.

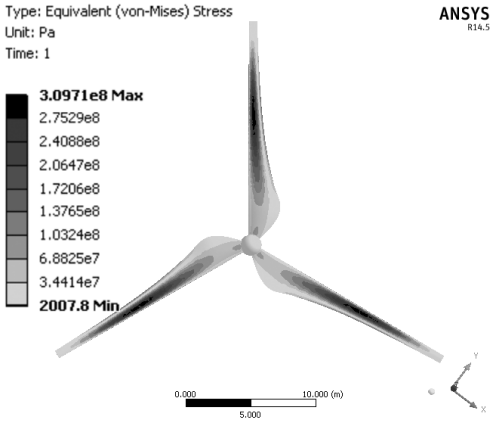

Fig.14. Distribution of Von Mises stress on the base blade

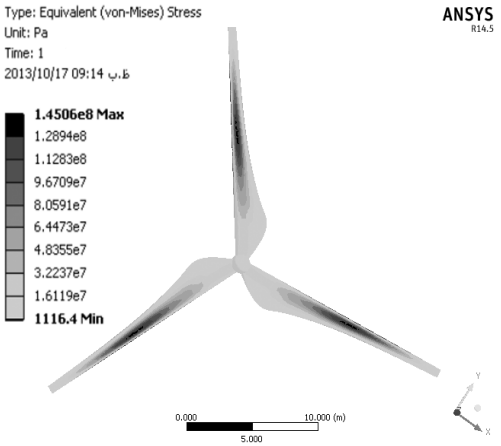

Fig.15. Distribution of Von Mises stress on the optimized blade

Figs.14 and 15 show the Von Mises stress distributions for the two blades. The distribution of Von Mises stress in the wider area is covered for the base blade and the maximum stress for the optimized blade is decreased 53%. This allows us that the optimized blade is made by weaker material or thiner blades.

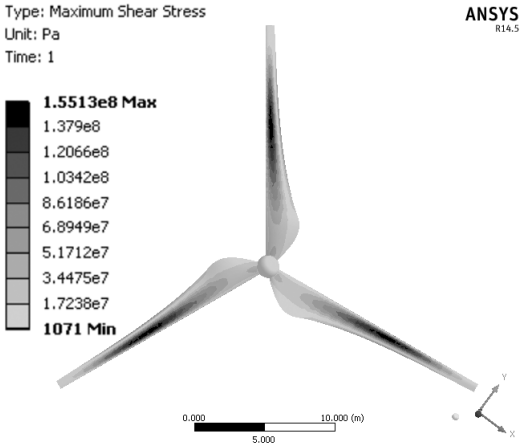

Fig.16. Distribution of maximum shear stress on the base blade

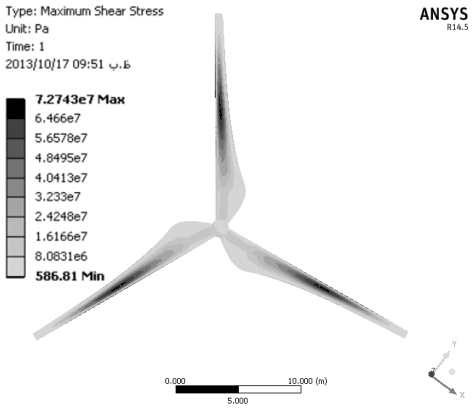

Fig.17. Distribution of maximum shear stress on the optimized blade

Figs. 16 and 17 show the maximum shear stress distribution on the base and optimized blades respectively. The maximum shear stress of optimized blade is less than base blade. In other words, it can withstand greater loads.

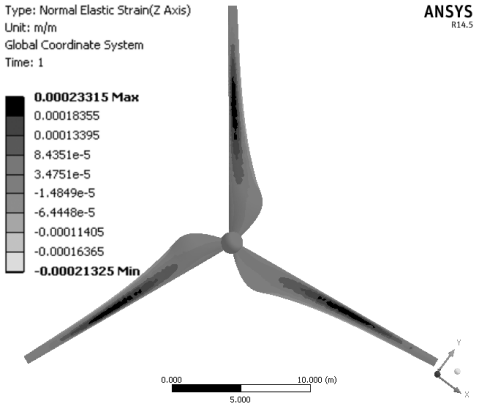

Fig. 18. Distribution of normal strain in the direction of the axis of rotation on the base blade

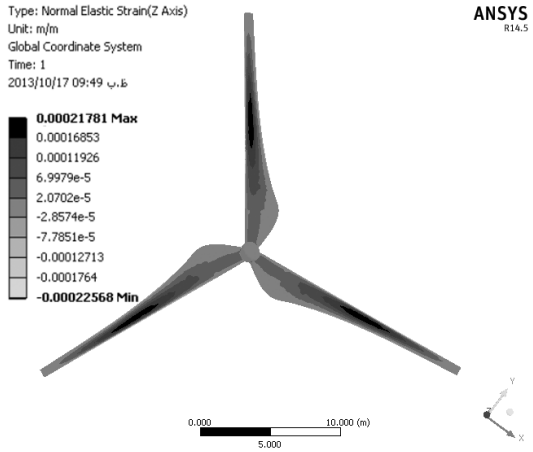

Fig. 19. Distribution of normal strain in the direction of the axis of rotation on the optimized blade

Figs.18 and 19 indicate the normal strain in the direction of the axis of rotation that is less about 6.57% in the optimized mode. This result shows that the axial normal stress is less for optimized blade. As can be seen the maximum axial normal strain is almost one third of the tip of the blade, that failure in this range is most of the rest .

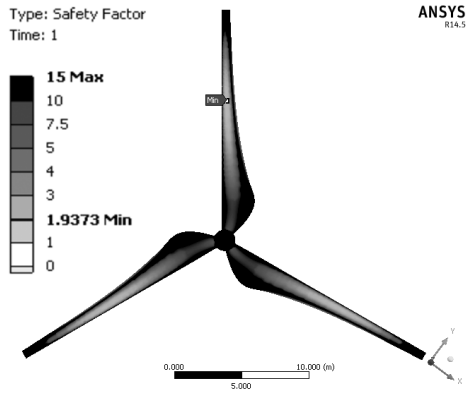

Fig.20. Distribution of factor of safty on base blade

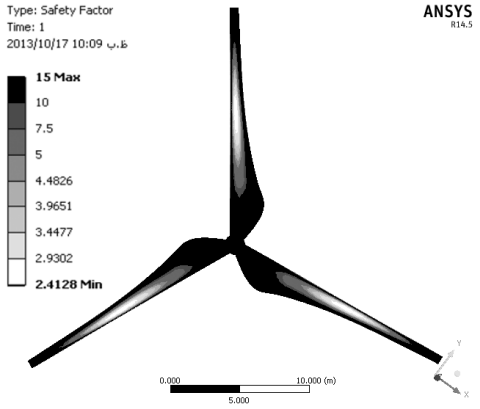

Fig.21. Distribution of factor of safty on optimized blade

Safety factor is the ratio of yield strength to allowable stress that always for every designe must be greater than one. Yield strength of the material does not depend on the load and shape but only to properties of the material dependent [14]. Here from Von Mises distortion energy theory have been reported. Observed that in this design and optimization that minimum safety factor in optimal mode increased 19.7% and indication of ensuring design.

4. Conclusion

In this article, two blades (optimized and base) of a horizontal axis wind turbine are compared from sight of aerodynamic and analysis of stress-strain. The shape of optimized blade be extracted by solving the viscous flow, Genetic Algorithms and Neural Networks,and after exerting aerodynamic forces, stress-strain analysis is performed on two blades.

The main points can be summarized as follow.

1) Power and Propulsion in aerodynamic analysis respectively 26 and 22 percent are increase in optimal mode.
2) The growth rates power and propulsion, in the optimized mode is greater than the base case.
3) In optimized blade, blade deformation along the radius is less than the base case, which makes the performance of blade from design mode less away.
4) The application of airfoils with high efficiency and good stall characteristics cause noticeable enhancement in wind turbine power factor.
5) In this simulation used less simplification for the analysis, and forces of pressure and viscosity have been put directly onto the nodes of blade.
6) In optimized blade, distribution of Von-Mises stress have decrease 53 percent, that makes the designer be able select the difference materials in a wider range or also decrease thickness of the blade. Thereby, the blades made lighter and the forces exerted on the shaft and bearing less, and more economical.
7) Safety factor in the optimum blade is greater than the base case.
8) Values of the stress-strain and deformation are reasonable and maximum stress values at critical points from the yield stress are not exceeded. The value of maximum principal stresses in the optimized blade is less than of the base blade and in the aerodynamic forces and bending more effectively.

Nomenclature

GA	Genetic Algorithm
CFD	Computational Fluid Dynamic
k	Turbulence Model Parameter
ε	Turbulence Model Parameter
τ	Shear Stress
c	Chord Length
AOA	Angle of Attack
ρ	Density
γ	shear strain
σ	Stress Tensor
ε	Strain Tensor
SIMPLE	Semi-Implicit Method For Pressure – Linked Equation
Re	Reynolds Number

References

[1] Min-SooJeonga, Sang-Woo Kima, In Leea, Seung-Jae Yoob, K.C. Parkc, d. " The impact of yaw error on aeroelastic characteristics of a horizontal axis wind turbine blade". 2013.

[2] Jong-Won Leea, Jun- SeongLeea, Jae-Hung Han," Aeroelastic analysis of wind turbine blades based on modified strip theory". 2012.

[3] Diego Cárdenasa, Hugo Elizaldeb, Piergiovanni Marzoccac, Sergio Gallegos," A coupled aeroelastic damage progression model for wind turbine blades".2012.

[4] Eelco Hoogedoorna, Gustaaf B. Jacobs," Aero-elastic behavior of a flexible blade for wind turbine application: A 2D computational study", 2008.

[5] C.A. Baxevanoua, P.K. Chaviaropoulosb, S.G. Voutsinasc, N.S. Vlachos," Evaluation study of a Navier–Stokes CFD aeroelastic model of wind turbine airfoils in classical flutter",2008.

[6] B.A. Freno,,P.G.A. Cizmas," A computationally efficient non-linear beam model", 2011.

[7] Martin Puterbaugh, AsfawBeyene," Parametric dependence of a morphing wind turbine blade on material elasticity", 2011.

[8] Andrea Dal Monte ,Marco RacitiCastelli , Ernesto Benini,"Multi-objective structural optimization of a HAWT composite blade",2013.

[9] Jin Chena, QuanWanga, Wen ZhongShenb, Xiaoping Panga, SonglinLi, "Structural optimization study of composite wind turbine blade", 2013.

[10] Neil Buckney, ,Alberto Pirrera, Steven D. Green, Paul M. Weaver,"Structural efficiency of a wind turbine blade",2013.

[11] M.H. Djavareshkian, A. Latifi Bidarouni, M.R. Saber " New Approach to High-Fidelity Aerodynamic Design Optimization of a Wind Turbine Blade" International Journal of Renewable Energy Research, Vol. 3, No. 3, pp. 725-734,2013.

[12] O. C. Zienkiewicz, The Finite Element Method in Engineering Science, New York, McGraw – Hill, 1971; W. Weaver, Jr. and P .R. Johnston. Finite Elements for Structural Analysis,Englewood Cliffs,NJ:Prentice-Hall,1984.

[13] Martin H. Sadd,"theory, applications, and numerics" Burlington, MA 01803, USA ,Linacre House, Jordan Hill ,Oxford OX2 8DP, UK,2009.

[14] Shigley ,Mischke , Budynas.1927 .Mechanical Engineering Design. 7th.ed.